Fraunhofer Institut
Techno- und
Wirtschaftsmathematik

Ph. Süss, K.-H. Küfer

Balancing control and simplicity: a variable aggregation method in intensity modulated radiation therapy planning

Berichte des Fraunhofer ITWM, Nr. 103 (2006)

ISSN 1434-9973

Bericht 103 (2006)

Die Veröffentlichungen in der Berichtsreihe des Fraunhofer ITWM können bezogen werden über:

Fraunhofer-Institut für Techno- und
Wirtschaftsmathematik ITWM
Fraunhofer-Platz 1

67663 Kaiserslautern
Germany

Telefon: +49 (0) 6 31/3 16 00-0
Telefax: +49 (0) 6 31/3 16 00-10 99
E-Mail: info@itwm.fraunhofer.de
Internet: www.itwm.fraunhofer.de

Vorwort

Das Tätigkeitsfeld des Fraunhofer-Instituts für Techno- und Wirtschaftsmathematik ITWM umfasst anwendungsnahe Grundlagenforschung, angewandte Forschung sowie Beratung und kundenspezifische Lösungen auf allen Gebieten, die für Techno- und Wirtschaftsmathematik bedeutsam sind.

In der Reihe »Berichte des Fraunhofer ITWM« soll die Arbeit des Instituts kontinuierlich einer interessierten Öffentlichkeit in Industrie, Wirtschaft und Wissenschaft vorgestellt werden. Durch die enge Verzahnung mit dem Fachbereich Mathematik der Universität Kaiserslautern sowie durch zahlreiche Kooperationen mit internationalen Institutionen und Hochschulen in den Bereichen Ausbildung und Forschung ist ein großes Potenzial für Forschungsberichte vorhanden. In die Berichtreihe sollen sowohl hervorragende Diplom- und Projektarbeiten und Dissertationen als auch Forschungsberichte der Institutsmitarbeiter und Institutsgäste zu aktuellen Fragen der Techno- und Wirtschaftsmathematik aufgenommen werden.

Darüber hinaus bietet die Reihe ein Forum für die Berichterstattung über die zahlreichen Kooperationsprojekte des Instituts mit Partnern aus Industrie und Wirtschaft.

Berichterstattung heißt hier Dokumentation des Transfers aktueller Ergebnisse aus mathematischer Forschungs- und Entwicklungsarbeit in industrielle Anwendungen und Softwareprodukte – und umgekehrt, denn Probleme der Praxis generieren neue interessante mathematische Fragestellungen.

Prof. Dr. Dieter Prätzel-Wolters
Institutsleiter

Kaiserslautern, im Juni 2001

Balancing control and simplicity: a variable aggregation method in intensity modulated radiation therapy planning

Philipp Süss*, Karl-Heinz Küfer

Department of Optimization
Fraunhofer Institute for Industrial Mathematics
Fraunhofer-Platz 1, 67663 Kaiserslautern, Germany

Abstract

It is commonly believed that not all degrees of freedom are needed to produce good solutions for the treatment planning problem in intensity modulated radiotherapy treatment (IMRT). However, typical methods to exploit this fact have either increased the complexity of the optimization problem or were heuristic in nature. In this work we introduce a technique based on adaptively refining variable clusters to successively attain better treatment plans. The approach creates approximate solutions based on smaller models that may get arbitrarily close to the optimal solution. Although the method is illustrated using a specific treatment planning model, the components constituting the variable clustering and the adaptive refinement are independent of the particular optimization problem.

*Corresponding author: *philipp.suess@itwm.fraunhofer.de*

1 Introduction

Radiotherapy is, besides surgery, the most important treatment option in clinical oncology. It is used with both curative and palliative intention, either solely or in combination with surgery and chemotherapy. The majority of radiotherapy patients is treated with high energetic photon beams. The radiation is produced by a linear accelerator and delivered to the patient by several beams coming from different directions (see figure 1). The goal of conformal radiation therapy is to deliver a high

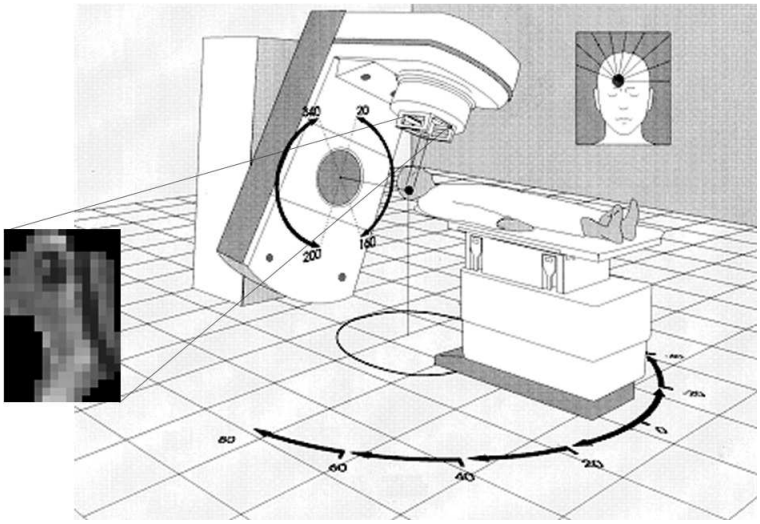

Figure 1: The gantry moves around the couch on which the patient lies. The couch position may also be changed to alter the beam directions.

and homogeneous dose to the tumor volumes while limiting the side-effects of this treatment. Aside from the risk of damaging critical healthy organs, there is also the risk of secondary cancer [3]. To better control the radiation received by the patient, several different methods have evolved to modulate the beam intensities from the gantry. First there was the *open field technique* where only the shape of each beam is adapted to the target volume. The intensity of the radiation throughout the beam's cross section is uniform or only modified by the use of pre-fabricated wedge filters. Over time the hardware improved and it was possible to fully modulate the intensity of each beam. *Intensity modulated radiation therapy* (IMRT) is realized by *multi-leaf collimators* (MLCs) (see figure 2). Parts of the beam surface are uncovered for individually chosen opening times while the rest of the area is covered by the leaves. The intensities emitted from these beams are described by *intensity maps* such as the one depicted on the left side of figure 1. One method to apply these intensity maps is to turn off the beam energy while the leaves of the MLC move. This is called *static* delivery. The alternative where the beam stays on during the application of one intensity map is the *dynamic* delivery. While both

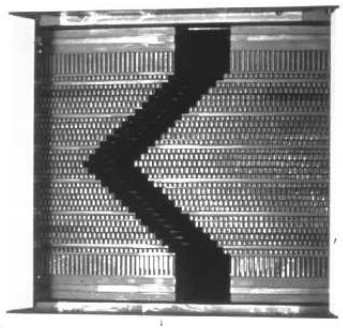

Figure 2: A Multileaf Collimator (MLC). The square opening is partially covered by leafs, each of which can be individually moved. Picture taken from [9].

are used in practice, the considerations in this paper are only relevant for the static method.

Finding suitable intensity maps given a set of beam directions and corresponding couch angles is the *treatment planning problem* in IMRT. We demand that the directions and couch angles are fixed because to find optimal directions is a global optimization problem. The variables of the treatment planning problem are therefore the intensity maps. Usually, the cross section of the beam is discretized on a regular grid with a resolution determined by the width of the collimator leaves. This corresponds to a discretization to fields of size typically less than or equal to 10 x 10 mm. Each small field is called a *beamlet*. The number of variables in a typical treatment planning problem with five to seven beam directions corresponds to several hundred beamlets. The aim to destroy cancerous cells while sparing healthy structures naturally lends itself to the formulation of a multicriteria optimization problem in which the dose in each tumor and each healthy structure is assessed with separate objective functions [15]. A decision-support system to select a treatment plan from the Pareto frontier of such a multicriteria approach is described in detail in [6].

This multicriteria approach provides control over the trade-off between overdosing healthy structures and destroying cancerous cells. However, it does not consider the time needed to deliver the intensity maps using an MLC. The risks of treatment errors due to patient movement and too much exposure to radiation increase with treatment time. An objective function that provides some control over this aspect was introduced in [2]. However, adding an objective function to the treatment planning problem also increases its complexity. When faced with a complicated case with many healthy structures close to the tumor volumes, significant computation time might be saved by disregarding the treatment time during optimization. Instead, the intensity maps are transformed before they are translated into MLC leaf configurations and delivered to the patient.

One such transformation is to reduce the number of different intensity levels in an intensity map. Experiments show that if the number of intensity levels decreases, the number of apertures can be expected to decrease also [5, 14]. This *stratification* can, for example, be performed for a given intensity map as shown in figure 3. However, this requires a solution to the planning problem. A reduction of the num-

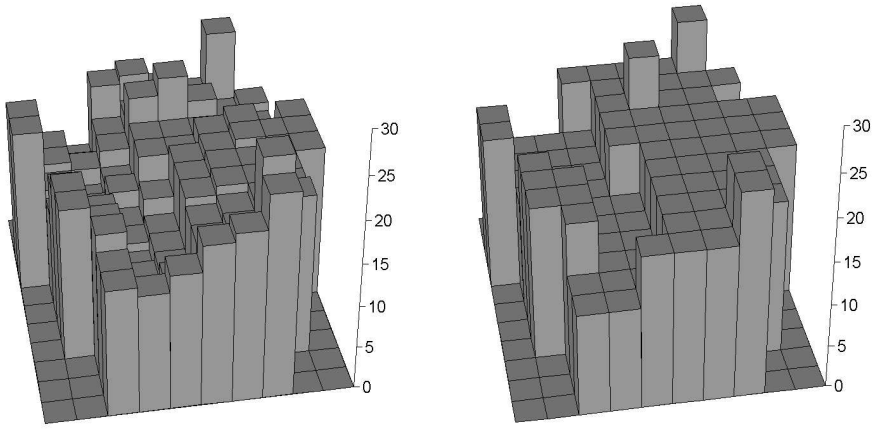

(a) Original intensity map (b) Stratified intensity map

Figure 3: The original intensity map was stratified to 5 distinct intensity values. The map in 3(a) needs 27 apertures, whereas the map in 3(b) needs only 5 apertures.

ber of variables in the treatment planning problem by requiring that some beamlets have the same intensity value is the *a priori* counterpart to stratification. The benefit of a priori stratification are simpler calculations by a reduction in the number of variables and a reduction in the number of apertures and a shorter treatment time because the plans are simpler. The cost is a limited control over the dose in the patient's body. The trade-off between the consequences of stratification must be carefully evaluated when planning a therapy.

Some attempts have been made to modify optimization algorithms for the treatment planning problem to reduce the number of apertures resulting from sequencing. Most notably, Alber and Nüsslin [1] have proposed an operator that modifies the solution at every fixed iterations during the optimization. This operator sets neighboring beamlets to equal intensities, which are then grouped to apertures. The intensity corresponding to all created apertures are then additional variables in the optimization. A different approach was taken by Keller-Reichenbecher et al [5]. Here, the solution is stratified to a small number of intensity levels every fixed number of iterations. Although the results presented in the latter approach indicate that the methods performs quite well, it remains a heuristic approach and does not in general converge to an optimal solution.

To address the goal of a short treatment time, the new objective function in [2] and the approach in [1] increased the complexity of the problem. The method in [5] retained the complexity of the original planning problem, but it is a heuristic. In this paper, we describe a method to first reduce the number of variables of the planning problem to a very small number. During the solver iterations, we adaptively add more degrees of freedom to refine the solution until it is acceptable. The planner may set a limit to the number of variables that are used and can control the resulting complexity of the intensity maps. By setting this limit equal to the number of variables in the treatment planning problem, this approach produces optimal solutions. Moreover, it is numerically verified that the adaptive refinement of the problem formulation based on clinically meaningful guidelines has a positive effect on the convergence of a solution mechanism.

In chapter 2 we motivate the idea of aggregating the variables by the dose computation necessary in IMRT planning. We also justify the use of a heuristic clustering procedure. In chapter 3 we introduce the clustering technique and demonstrate its applicability on an artificial example and on a clinical prostate case. We also specify a treatment planning problem formulation for the prostate case which will serve as an illustration for the techniques later. In chapter 4, the refinement strategy is proposed and carried out for the prostate case. Numerical results about the solver progress and the comparison of the solutions obtained by the aggregation and refinement and the original formulation are made. Chapter 5 concludes this paper.

2 Dose computation and variable aggregation

As it was mentioned, the intensity maps are discretized on a regular grid to a set of beamlets. The patient's body is also discretized into small volume elements called *voxels* to simplify the computation of the dose received by each small volume part. The slices of the CT scan imply a natural dissection in the z-direction. Together with a further sectioning of the x-y plane, the voxels typically are of dimensions of a few millimeters. As a consequences of these discretizations and the superposition principle of dose deposits in photon therapy, the dose distribution over the voxels can be calculated by the matrix multiplication

$$\mathbf{d} = \mathbf{P} \cdot \mathbf{x}, \tag{1}$$

where $\mathbf{d}$ is the m-dimensional vector of dose values for all voxels, the matrix $\mathbf{P}$ is the *dose information matrix*, and the n-dimensional vector $\mathbf{x}$ are the intensities of the beamlets over all beams, written as one column vector. The entry p_{ji} of the dose information matrix represents the contribution of the ith beamlet to the absorbed dose in the jth voxel under unit intensity. There are several methods to estimate these values. They might be calculated using the pencil beam approach, a superposition algorithm, or some Monte Carlo method. In this paper we do not

discuss this important issue - the interested reader is referred to the books by Webb [12, 13]. We assume that $\mathbf{P}$ is given in some satisfactory way. Note that the rows of $\mathbf{P}$ correspond to the voxels and the columns to the beamlets. Therefore, $\mathbf{P}$ typically has a little over one million rows and several hundred columns. Moreover, the matrix is sparse - often only 10% of the entries are positive. The reason is that one beamlet only hits a small portion of voxels compared to the entire volume. The dose calculation takes significant time in an iterative optimization algorithm to determine the intensity maps - even when techniques to exploit the sparsity of $\mathbf{P}$ are used. Further, as MLC hardware becomes even more sophisticated, the leaves will become thinner, and the number of columns of $\mathbf{P}$ will increase in the future.

A numeric technique to reduce the number of rows of $\mathbf{P}$ using an adaptive clustering method was presented in [8]. Neighboring voxels belonging to the same organs or tumors are treated as groups if their dose deposits are "similar". The optimization is carried out on these clusters of voxels with a dose information matrix that has relatively few rows. The largest errors due to the clustering are identified and the clusters broken up to attain a refined description of the body. This iteration between optimization and refinement continues until the clustering error is below a threshold. In this paper, we focus on the aggregation of variables, so we are interested in reducing the number of columns of $\mathbf{P}$.

To reduce the degrees of freedom of the treatment planning problem means to constrain some of the beamlets to have equal intensity values. Imagine that the beamlets are partitioned into L groups $\mathcal{B}_1, \ldots, \mathcal{B}_L$, and each group of beamlets has their own intensity ℓ_b. Thus, $x_i = \ell_b$ for all beamlets i belonging to group $\mathcal{B}_b$. This means, the dose calculation (1) can be written as

$$d_j = \sum_{i=1}^{n} p_{ji} \cdot x_i = \sum_{b=1}^{L} \sum_{i \in \mathcal{B}_b} p_{ji} \cdot x_i = \sum_{b=1}^{L} \ell_b \sum_{i \in \mathcal{B}_b} p_{ji}, \quad \forall j = 1, \ldots, m. \tag{2}$$

Aggregating the variables in the treatment planning problem effectively reduces the size of $\mathbf{P}$ by summing up all columns that correspond to beamlets with identical intensity values. To code the allocation of beamlets to same groups, we introduce the $n \times L$ matrix $\mathbf{A}$ with entries

$$a_{ib} = \begin{cases} 1 & \text{if beamlet } i \text{ is allocated to group } b \\ 0 & \text{else} \end{cases}$$

The dose calculation (2) can then be written as $\mathbf{d} = \mathbf{P} \cdot \mathbf{A} \cdot \boldsymbol{\ell}$, with $\boldsymbol{\ell}$ as the vector of all group intensities. The "small dose information matrix" $\mathbf{P} \cdot \mathbf{A}$ makes the computation of $\mathbf{d}$ much faster if $L \ll n$.

If the number of different intensity levels L is fixed, we can formulate the allocation problem to find $\mathbf{A}$ as an optimization problem to minimize a metric that describes the error due to the aggregation. In other words, right-multiplying $\mathbf{A}$ to $\mathbf{P}$ should keep the norm $\|\mathbf{d} - \mathbf{P} \cdot \mathbf{A} \cdot \boldsymbol{\ell}\|_q$ for $q \geq 1$ and any given dose $\mathbf{d}$ and intensities $\boldsymbol{\ell}$ small.

Problem 2.1 (Allocation problem)
Given a dose distribution $\mathbf{d}$*, a dose information matrix* $\mathbf{P}$ *and a set of group intensities* $\boldsymbol{\ell}$*, find an allocation* $\mathbf{A}$ *that approximates the resulting evaluation of dose distribution as close as possible under the norm* $\|\cdot\|_q$ *for* $q \geq 1$*:*

$$\begin{aligned} \min_{\mathbf{A}} \quad & \|\mathbf{d} - \mathbf{P}\cdot\mathbf{A}\cdot\boldsymbol{\ell}\|_q \\ \sum_{b=1}^{L} a_{ib} &= 1 \qquad \forall\, i = 1,\ldots,n \\ a_{ib} &\in \{0,1\} \quad \forall\, i = 1,\ldots,n, \quad b = 1,\ldots,L \end{aligned}$$

Note that the constraints in Problem 2.1 produce a partition of the beamlets. Unfortunately, the Allocation problem is NP-hard.

To see that the Allocation problem is hard, we reduce PARTITION to an instance of Problem 2.1. Let $k_1,\ldots,k_n$ be a set of positive integers and $g = \frac{1}{2}\sum_{i=1}^{n} k_i$. PARTITION asks if there is a partition of the integers into subsets S_1 and S_2 such that $\sum_{i\in S_j} k_i = g$ for $j = 1, 2$. Now consider the following Allocation problem:

$$\begin{aligned} \min_{\mathbf{A}} \quad & \left\| \begin{bmatrix} g \\ g \end{bmatrix} - \begin{bmatrix} k_1 & k_2 & \ldots & k_n \\ k_1 & k_2 & \ldots & k_n \end{bmatrix} \begin{bmatrix} a_{11} & a_{12} \\ a_{21} & a_{22} \\ \vdots & \vdots \\ a_{n1} & a_{n2} \end{bmatrix} \begin{bmatrix} 1 \\ 1 \end{bmatrix} \right\|_q \qquad (3) \\ a_{i1} + a_{i2} &= 1 \qquad i = 1,\ldots,n \\ a_{ib} &\in \{0,1\} \quad i = 1,\ldots,n,\ b = 1,2 \end{aligned}$$

If the optimal objective function value (3) is 0 for any $q \geq 1$, then PARTITION is answered with yes, and no otherwise. This is the Allocation problem with $\mathbf{d} = \begin{bmatrix} g & g \end{bmatrix}^T$, $\mathbf{P}$ with the set of integers $k_1,\ldots,k_n$ as row vectors, and the group intensities $\boldsymbol{\ell}$ given by $\mathbf{1}$, the vector of all 1s. This result discourages a search for the optimal aggregation. The alternative is to develop a method that produces solutions of acceptable quality.

Note that if two columns of $\mathbf{P}$ are "similar", meaning the positive entries hit voxels belonging to the same structures with similar contributions, it may be expected that the optimal intensities corresponding to the two beamlets are similar as well. That is, we would like to group together those beamlets with similar impact on the dose distribution $\mathbf{d}$. Grouping similar objects is achieved by clustering methods [4]. In the following chapter, we derive a clustering algorithm to group similar beamlets.

3 Beamlet clustering and implications

The ingredients for a clustering method are a measure of similarity between objects and between objects and clusters, and an algorithm to group the objects based on

these similarities. Instead of maximizing the similarity between objects inside a cluster, the *dis*similarity could be minimized. A simple measure of dissimilarity of objects that are characterized by a vector of real numbers are the distance metrics

$$\text{dist}_q(\mathbf{x}, \mathbf{y}) := \sqrt[q]{\sum_i |x_i - y_i|^q}, \tag{4}$$

for $q \geq 1$. For $q = 1$, (4) is the *rectilinear* or *Manhattan metric*, and for $q = 2$, (4) becomes the *Euclidean metric*. We will use $q = 2$ and take "dist" without the subscript q to mean the Euclidean metric from here on. A cluster will be represented by an average over all columns that are grouped to it. This representative is given by

$$\boldsymbol{\mu}_k = \frac{1}{|\mathcal{B}_k|} \sum_{i \in \mathcal{B}_k} \mathbf{P_i},$$

where $\mathbf{P_i}$ is the ith column of $\mathbf{P}$.

A first attempt to characterize the beamlets might be to use the columns of $\mathbf{P}$. There are, however, two disadvantages associated with taking the entire "information" of each beamlet. First, evaluating the distance (4) between two beamlets takes a long time because potentially many entries have to be compared. This calculation becomes even more tedious as clusters grow in size because a vector of averages over sparse columns is in general less sparse. The other disadvantage is that the distance measure does not "discriminate" enough if the original columns are used. The positive entries in $\mathbf{P}$ range from the orders 10^{-5} to 10^2, and large values will have a dominating effect on the distance. As a result, only large deviations between two objects determine their dissimilarity and small entries are largely ignored. In IMRT, however, it is especially the many small contributions that add up to significant doses that can be exploited to shape the dose distribution. Therefore, a different characteristic for beamlets and cluster representatives must be found.

Better clusters can be expected when the information contained in the columns of $\mathbf{P}$ are condensed on an organ level. The contribution of a beamlet to a specific organ is given by the entries in the rows corresponding to voxels of that organ. From a statistics viewpoint, if these entries are seen as random variables, their *moments* suffice to characterize the beamlets. The kth moment of a random variable Y is given by the expected value of the kth power of Y, $E\left(Y^k\right)$. We will characterize the beamlets and cluster representations by a vector of moments for each organ in the patient body. We limit the number of moments to at most 3, since higher moments are typically only of theoretical value [11, Chapter 3.9]. Thus, the vectors characterizing our objects only contain (number of organs $\times$ number of moments ≈ 10 to 20) entries and could look like the following if 2 moments are used:

$$\mathbf{c}_i = \begin{bmatrix} c_{s_1\,1}(i) & c_{s_1\,2}(i) & c_{s_2\,1}(i) & c_{s_2\,2}(i) & c_{s_3\,1}(i) & \dots \end{bmatrix}^T,$$

where the entry $c_{s_1\,h}(i)$ denotes the hth moment of the contributions of beamlet i to the organ s_1 given by

$$c_{s_1\,h}(i) = \frac{1}{|s_1|} \sum_{j \in s_1} p_{ji}^h. \tag{5}$$

The entries of the other organs are similar to (5).

Now that we have decided on the dissimilarity measure for beamlets and cluster representatives, we need a method to group the beamlets into clusters. Because we fixed the number of clusters in Problem 2.1, we use the K-means algorithm 3.1 to aggregate the variables.

Algorithm 3.1 K-means algorithm adapted from [4]

Procedure: $KMeans$

Input: Characteristic vectors $\mathbf{c}_i$, $i = 1, \ldots, n$, number of clusters K, distance measure "dist"

Output: allocation $\mathbf{A}$

Step 1: Produce initial clusters $1, 2, \ldots, K$ and allocation $\mathbf{A}$ and compute the cluster means $\boldsymbol{\mu}_1, \ldots, \boldsymbol{\mu}_K$.

Step 2: For beamlet $i = 1$, compute for every cluster k the increase in error in transferring this beamlet from cluster $a(1)$ to cluster k given by $|k| \cdot \frac{\text{dist}(\mathbf{c}_i, \boldsymbol{\mu}_k)}{(|k|+1)} - |a(i)| \cdot \frac{\text{dist}(\mathbf{c}_i, \boldsymbol{\mu}_{a(i)})}{(|a(i)|-1)}$, where $|k|$ denotes the cluster size of cluster k, and $a(i) = \{b : a_{ib} = 1\}$ denotes the cluster to which beamlet i is assigned to. If the minimum of this quantity over all $k \neq a(i)$ is negative, transfer the beamlet i from cluster $a(i)$ to this minimal k, adjust the cluster means of $a(i)$ and k, and set $a(i) := k$.

Step 3: Repeat Step 2 for $i = 2, \ldots, n$.

Step 4: If no movement of a beamlet from one cluster to another occurs, stop. Otherwise, return to Step 2.

The characteristic vectors are the collections of moments of organ contributions, and the distance measure is the Euclidean. The cluster means are determined by adding the dose contributions of newly added or removed beamlets and is the most time-consuming operation of $KMeans$. Algorithm 3.1 is performed separately for each beam to ensure that exactly L clusters represent the beamlets of each direction. One method to obtain an initial clustering for Step 1 is to randomly assign beamlets to the K clusters. This also has the advantage that it produces different starting points for $KMeans$, each leading to a different locally optimal allocation. Typically the method runs fast enough so that the clustering can be performed several times with different starting points. The clustering with the smallest error is taken as the final aggregation.

3.1 Case 1: Artificial example

To demonstrate the basic effects of this type of variable aggregation, a simple, artificial case was created. Figure 4 shows one of the transversal slices of this case. The "body" is a large cube, and there are only three relevant structures. The cuboid at the bottom inside the body represents the tumor volume, and the other two structures resemble healthy organs. Five beam directions were chosen and the beamlets clustered to only 2 or 3 groups to illustrate the effect of this type of variable aggregation technique.

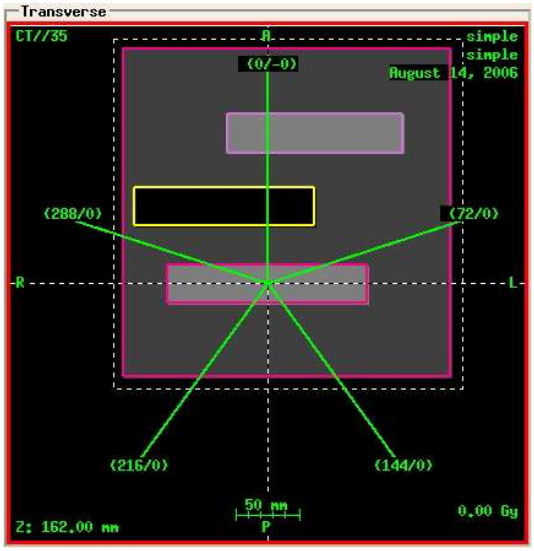

Figure 4: This shows the view of a transversal cut of the artificial example in the planning software KonRad (developed by the DKFZ in Heidelberg). The tumor is the cuboid where the beam directions intersect.

The tumor and the organs have size 20 x 4 x 16 cm. The voxel sizes were set to 1 x 1 x 3 mm. This corresponds to a total of 363,825 voxels for this case. Over all 5 beams, a total of 441 beamlets actually hit the tumor volume and constitute the degrees of freedom in the treatment planning problem for this artificial case. The number of positive entries in $\mathbf{P}$ is about 14% of all entries in the matrix. We refer to the beam directions by their angles. Starting from the beam entering from the top of figure 4 with angle 0, the directions are separated by 72 degrees.

The beamlets of the directions 0 and 288 degrees were grouped in 3 clusters, and the rest of the directions were clustered in 2 groups. As a result, the matrix $\mathbf{P} \cdot \mathbf{A}$ has only 12 columns, and about 36% of its entries are positive. Calculating the characteristic vectors for all beamlets and the clustering procedure took a total of about 2.4 seconds per beam on a 2.2 GHz processor. Figure 5(a) shows the cluster number of each beamlet in the intensity map corresponding to beam 0. It was

natural to choose 3 clusters because the back-projection of the structures on the

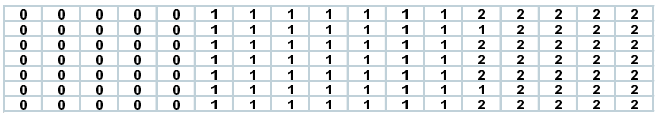

(a) Beam 0

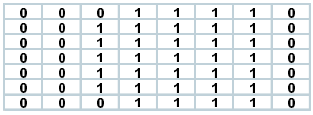

(b) Beam 72

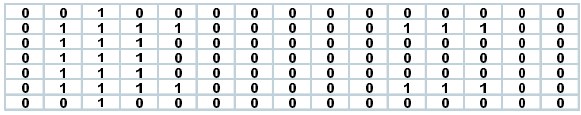

(c) Beam 144

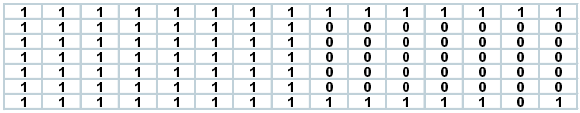

(d) Beam 216

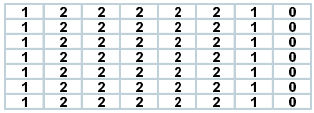

(e) Beam 288

Figure 5: Cluster numbers of the beamlets in each beam for the artificial example. The beams are of different size because the planning software automatically eliminates those beamlets that do not hit the tumor.

surface of the beam can be parted in three: one area in the middle where both organs are in front of the tumor, and two areas where only one is in the way of the beam. Note that the clustering algorithm has no information about the location of the beamlets on the beam surface - they were clustered solely based on the information about their contributions to the structures. The other beam directions showed similar geometric back-projections. The clusters in beam 216 (figure 5(d)), for example, also resemble the projection of the structures on the beam: the area on the beam where only the farthest structure is hit constitutes a separate cluster of beamlets.

3.2 Case 2: Clinical prostate example

While the first artificial example demonstrates that the clustering method based on organ information is in principle capable of identifying different critical regions on the surface of the beam, this does not yet warrant a successful application to real cases. In this section, a prostate case is studied and the variables are aggregated. We will additionally formulate a treatment planning problem and compare the results from the original formulation with the solution to the aggregated problem. We delay the discussion of improving the aggregated solution until chapter 4.

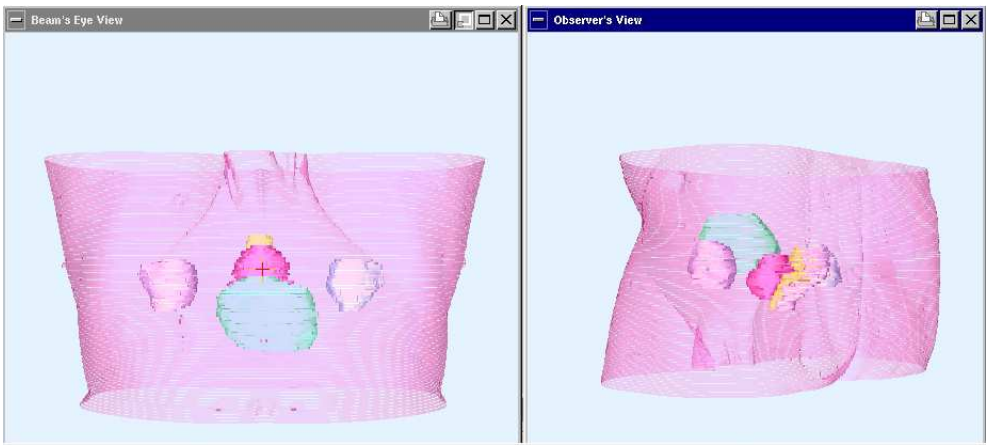

Figure 6: This view is taken from VIRTUOS (developed by the DKFZ in Heidelberg) and shows the three-dimensional representation of the patient's body. The left window shows the view from the direction of beam 0.

In this case, the prostate and the seminal vesicles are the target volumes. They compose the structure marked with the crosshairs in the left window of figure 6. The structure in front of the prostate is the bladder, and behind the prostate, the rectal walls (anterior and posterior) are segmented separately. Finally, the femoral heads are also included as critical structures in this case to limit the dose absorbed by lateral beam directions.

The dose information matrix consists of 799,200 rows and 173 columns. Again, 5 equiangular beam directions were chosen. There are 13,414,539 positive entries in $\mathbf{P}$, which is 9.7% of all entries. The number of clusters was set to 4 for beam 0 and 5 for the rest. Determining the characteristics of all beamlets and aggregating them took a total of only 2 seconds per beam on a 2.2 GHz processor. The clusters are depicted in figure 7. Again, the clusters closely resemble projections of the structures on the beam. In beam 0, for example, the beamlets corresponding to cluster 1 hit the prostate and both the anterior rectal wall and the posterior rectal wall. Cluster 2 are those beamlets where either only one or no rectal wall is hit. The beamlets in clusters 0 and 3, finally, have to shoot through the bladder and also hit both rectal walls behind the target. Cluster 0 hits the prostate and the beamlets in cluster 3 hit the seminal vesicles. Similar observations can be made for the other beam directions. As a result of the variable aggregation, $\mathbf{P} \cdot \mathbf{A}$ contains only 24 columns, and the percentage of positive entries increased to 17.6%.

To illustrate the loss in control we imposed, we now compare the original and aggregated solution to the following planning problem. The objective functions for the healthy structures are based on the equivalent uniform dose (EUD) concept

	2	2	1	1	2	
	2	1	1	1	2	
	2	1	1	1	2	2
2	2	1	1	1	2	2
3	0	0	0	0	0	3
3	3	3	3	3	3	3

(a) Beam 0

2	2	2	0	0		
2	1	1	1	0	0	
2	1	1	1	3	0	
2	2	1	3	3	3	
	2	1	4	4	4	3
			3	4	3	0

(b) Beam 72

0	0	1	3	3		
0	0	1	1	3	3	
0	1	1	1	1	3	
0	0	0	1	1	4	
0	2	2	2	2	4	4
	0	2	2	4	4	

(c) Beam 144

		0	2	3	3	1
	0	0	2	3	3	3
	0	2	2	3	3	3
	0	2	3	3	3	1
0	4	4	4	4	4	1
0	2	1	1	1	1	

(d) Beam 216

		0	0	3	3	3
	0	0	2	2	2	3
	0	1	2	2	2	3
	1	1	1	2	3	3
	4	4	4	3	3	
0	1	1	1			

(e) Beam 288

Figure 7: Cluster numbers of the beamlets in each beam. Some beamlets are "switched off" because the planning software automatically eliminates those beamlets that do not hit the tumor.

[7]. They are of the form

$$f_{\text{EUD},s}(\mathbf{d}) = \alpha_s \cdot d_{\text{ref},s}^{-1} \cdot \Big(|s|^{-1} \cdot \sum_{j \in s} d_j^{p_s} \Big)^{p_s^{-1}} + (1-\alpha_s) \cdot d_{\text{ref},s}^{-1} \cdot \Big(|s|^{-1} \cdot \sum_{j \in s} d_j^{q_s} \Big)^{q_s^{-1}}, \tag{6}$$

where s denotes the corresponding organ, $|s|$ is the number of voxels in that organ, α_s a weight between 0 and 1, $d_{\text{ref},s}$ a reference dose value for organ s, and p_s and q_s are organ-specific modeling parameters (≥ 1). If p_s and q_s are relatively small, the smaller dose values d_j in s are emphasized more. By combining two EUD-type functions, it is possible to model the objective function according to the flexible max-and-mean EUD concept introduced in [10]. The reference dose values $d_{\text{ref},s}$ are included to ensure comparability between the objective functions for different organs. The planner must choose the reference doses according to the statement "a dose of d_{ref,s_1} in structure s_1 is of same importance to me as a dose of d_{ref,s_2} in structure s_2". Note that the scale of these reference values does not matter - only the relative magnitudes to each other.

The objective functions for the tumor volumes are given by

$$f_{\text{cur}}(\mathbf{d}) = d_{\text{cur}}^{-1} \cdot (|t|^{-1} \cdot \sum_{j \in t} \max \{0, d_{\text{cur}} - d_j\}^{q_{\text{cur}}})^{q_{\text{cur}}^{-1}} \tag{7}$$

to evaluate a lower bound for the target dose, and

$$f_{\text{hom}}(\mathbf{d}) = d_{\text{hom}}^{-1} \cdot (|t|^{-1} \cdot \sum_{j \in t} \max \{0, d_j - d_{\text{hom}}\}^{q_{\text{hom}}})^{q_{\text{hom}}^{-1}} \tag{8}$$

with d_{hom} slightly larger than d_{cur} to ensure that the dose is homogeneous in the tumor volume.

The values for each parameter of the functions (6)-(8) are given in the following table.

Structure s	$d_{\text{ref},s}$	p_s	q_s	α_s
tissue	45	2	2	-
right femoral head	50	3	8	0.3
left femoral head	50	3	8	0.3
anterior rectal wall	40	3	8	0.75
posterior rectal wall	25	3	8	0.25
bladder	30	3	8	0.35

The values for the tumor volumes are $d_{\text{cur}} = 76$ and $d_{\text{hom}} = 80$. The values for q_{cur} and q_{hom} are both 4.

The scalarized multicriteria optimization formulation to solve the treatment planning problem can now be stated:

Problem 3.1 (Scalarized treatment planning problem)

$$\begin{aligned}
\min_{\mathbf{x}} \quad & z & & \\
\mathbf{d} &= \mathbf{P} \cdot \mathbf{x} & & \\
f_{EUD,s}(\mathbf{d}) &\leq z & & \forall \textit{critical structures } s \\
f_{cur}(\mathbf{d}) - 0.5 &\leq 0 & & \\
f_{hom}(\mathbf{d}) - 0.5 &\leq 0 & & \\
\mathbf{x} &\geq \mathbf{0} & &
\end{aligned}$$

The constraints $f_{\text{cur}}(\mathbf{d})$, $f_{\text{hom}}(\mathbf{d}) \leq 0.5$ on the tumor volumes largely prevent under-shooting d_{cur} and exceeding d_{hom}. There is no method to test a priori if these constraints can be met. In addition, we would like to use the solution to one aggregated problem as a starting solution for the next refined problem as described in the next chapter. That is, the solver used must be able to cope with infeasible as well as feasible iterates. For this reason, problem 3.1 is solved by a penalty sequential linear programming solver.

One graphical output of the quality of a plan is the dose-volume histogram (DVH). These histograms display the percentage of a structure that receives at least a certain dose over the relevant dose interval. The DVH for the original problem is given in figure 8. All calculations were done on the same 2.2 GHz processor to ensure

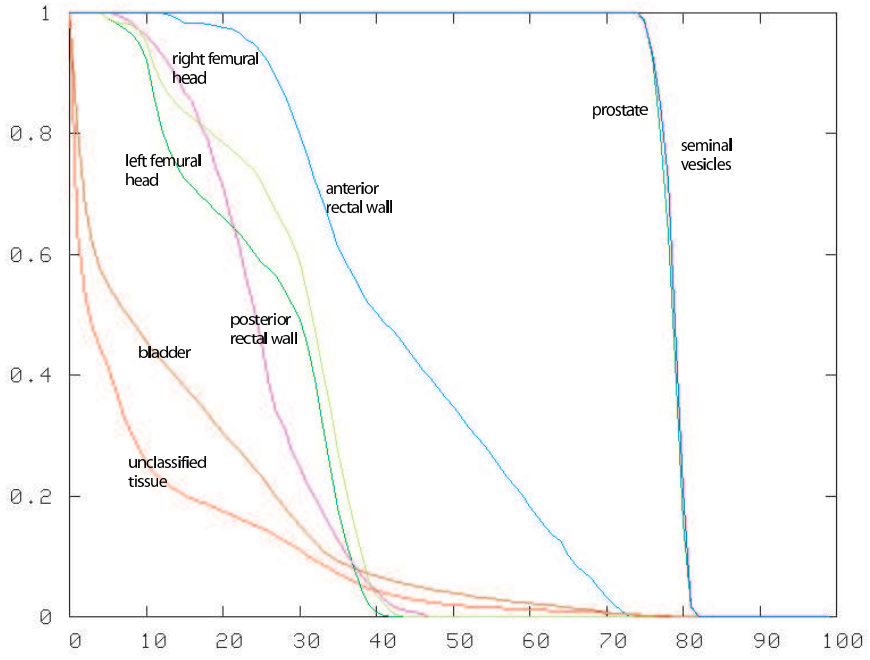

Figure 8: DVH for the original solution.

comparability. The solver needed 23 minutes to obtain this solution. The DVH of the solution on the aggregated variables is depicted in 9 and the solver only needed 3 and a halve minutes. At first glance, it is obvious that the solution to the aggregated problem is not feasible. This may be expected as the degrees of freedom in the planning problem were severely reduced. However, there is a striking similarity in the DVH curves for the organs at risk in both histograms. The following table containing the EUD values (not normalized by their reference dose) also shows this.

Structure s	original $f_{\text{EUD},s}$	aggregated $f_{\text{EUD},s}$	% deterioration
right femoral head	31.14	29.90	-4.00
left femoral head	32.92	32.97	0.15
anterior rectal wall	49.92	47.46	-4.93
posterior rectal wall	30.65	32.31	5.42
bladder	37.80	38.42	1.64

The following comparison of the true minimum dose in the tumor volumes indicate

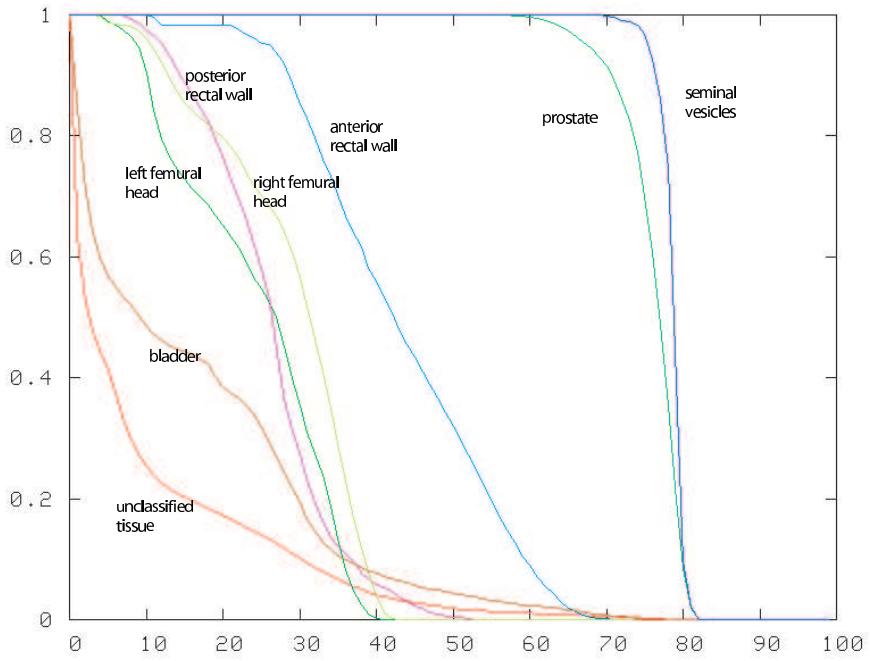

Figure 9: DVH for the aggregated solution.

that the solution to the aggregated problem is not feasible. In fact, both demands on the curative doses for the prostate and the seminal vesicles are not satisfied.

Target	original min dose	aggregated min dose
Prostate	73.41	57.18
Seminal vesicles	74.41	49.47

The constraints pertaining to the maximum doses in the targets, however, can be met as the maxima of each volume for both solutions indicate:

Target	original max dose	aggregated max dose
Prostate	81.73	81.79
Seminal vesicles	81.42	81.52

It is, of course, not surprising that reducing the number of variables from 173 to only 24 may not produce feasible solutions. Some more variables in the planning problem are definitely needed. An iterative procedure to decide which variables to "free" for a subsequent optimization problem is the topic of the next chapter.

4 Adaptive control and refinement of clusters

In chapter 3, a method to aggregate the variables of the treatment planning problem was presented. In this section, we cover the refinement of variable clusters. It

is expected that the quality of a solution can deteriorate rather strongly or may not even be feasible when the number of clusters is small. Hence, a mechanism to break up existing clusters at stages in the algorithm must be implemented to improve the solution of an aggregated problem. Similar to the voxel clustering technique in [8], we call such a method an *adaptive refinement*. In principle, the adaptive refinement creates a series of aggregated optimization problems starting from the first variable cluster, and successively breaks existing clusters in two *child clusters*. The treatment planning problem with the increased number of beamlet clusters is solved again and the objective function values are checked. An upper limit of how many variables can be freed this way serves as a stopping criterion. Of course, if the solution is still infeasible or the planner is not satisfied with this result, the procedure may be continued.

We will first introduce an idea to identify child clusters of existing aggregations based on the reference doses for each organ. Then we elaborate on how to control the iterations in the refinement. The prostate case of the previous chapter serves as a continuing illustration of the methods proposed in this chapter.

The critical question in a disaggregation procedure is which variables to free from existing clusters. We will make this decision based on the characteristics of the beamlets. In every iteration we identify one organ S that has an unfavorable dose distribution. Then all the clusters are searched and those beamlets with significant influence on the selected organ are separated into a new cluster. A limit on how many clusters are broken up this way is one of the control parameters of the refinement. To prevent moving too many beamlets into a single new cluster, the new clusters are constrained to contain only as many entries as the average cluster size of the old clusters. The procedure $Refinement\_Iteration$ is given in detail in algorithm 4.1.

In Step 1 of each refinement iteration, the cluster errors regarding the target organ are evaluated and the worst clusters identified. These worst clusters all contain beamlets that could be used to better control the dose distribution in S. Those beamlets are identified in Step 2 of $Refinement\_Iteration$ and separated into new clusters. Since problem 3.1 demands to minimize the maximum EUD normalized by the reference doses, it is natural to pick that organ for which the maximum is attained as S.

The last choice that remains is how to choose the parameters of the refinement iteration. How many clusters should be formed in each iteration, and how many iterations should be done? One refinement iteration does not take much time because only the characteristic vectors of beamlets and clusters are compared. Each refined formulation of the treatment planning problem has to be resolved. The solution to the previous formulation should be an excellent starting point for the new problem and the refined solution should be found in a few solver iterations. Since this can all be achieved in little time, the number of clusters to be broken up in algorithm 4.1 can be set rather low - say 20 clusters over all beams.

Algorithm 4.1 Adaptive refinement iteration

Procedure: $Refinement\_Iteration$

Input: Characteristic vectors $\mathbf{c}_i$, $i = 1, \ldots, n$ of all beamlets, allocation $\mathbf{A} \in \mathbb{B}^{n \times K}$ of beamlets to clusters, cluster means $\boldsymbol{\mu}(1), \ldots, \boldsymbol{\mu}(K)$, average cluster size t_{ave}, target organ S, number of clusters d to break up

Output: new allocation $\mathbf{A}^N$, new cluster means $\boldsymbol{\mu}(1), \boldsymbol{\mu}(2), \ldots$

Step 1: For each cluster k that hits S, compute the clustering error of target organ S given by $\sum_h \left(\sum_{i \in k} (c_{S\,h}(i) - \mu_{S\,h}(k))^2 \right)^{h^{-1}}$, where h denotes the degree of the moment and rank the clusters in descending order of these errors.

Step 2: For the worst d clusters found, allocate all beamlets in those clusters that have a higher contribution to S than its cluster mean to a new cluster:

```
n := 1    // counter for newly created clusters
for k := 1 to d    // consider the worst clusters
    for all beamlets i ∈ k
        if c_{S h}(i) > μ_{S h}(k) then
            a^N(i) := K + n    // separate this beamlet from k
        else
            a^N(i) := a(i)
        end if
        if cluster K + n contains more than t_ave beamlets
            n := n + 1
        end if
    next beamlet i
next cluster k
```

As there exists a lot of empirical evidence that not many degrees of freedom are necessary to produce treatment plans of good quality, the limit of how many variables to end the refinement procedure can be set rather low initially. A simple refinement strategy is then to choose a low threshold for the number of variables (say 60% of the number of beamlets). Once the number of variables is above this threshold, the refinement is only continued if the solution is not yet feasible.

We now illustrate the refinement strategy using the prostate case we began in the previous chapter. Starting from the solution in chapter 3, the refinement is carried out using the following rules:

1. The organ to refine is the one for which the maximum (normalized) EUD is realized.
2. If an organ is refined for two consecutive iterations, it can't be refined in the next iteration.
3. In every iteration, 20 clusters are broken up.

4. Stop with the first feasible solution after the number of variables is above 60% of all beamlets.

Rule 2 is included to avoid that on organ is refined too aggressively. The following table indicates the progress of the refinement. The first row is the solution from the previous chapter. The third column indicates the time the solver has taken up to that point.

Ref.	organ	acc. solver time	number of variables	feasible?
0		3 m 38 s	24 (14%)	NO
1	post. rectal wall	6 m 23 s	45 (26%)	NO
2	bladder	9 m 13 s	65 (38%)	NO
3	ant. rectal wall	12 m 10 s	84 (49%)	NO
4	ant. rectal wall	15 m 14 s	108 (62%)	NO
5	bladder	18 m 26 s	133 (77%)	YES

The process stopped after about 18 and a halve minutes, and it took over 4 minutes less time than the original problem formulation. The DVH of the last refinement are shown in figure 10. Perhaps the most striking difference is in the curves pertaining

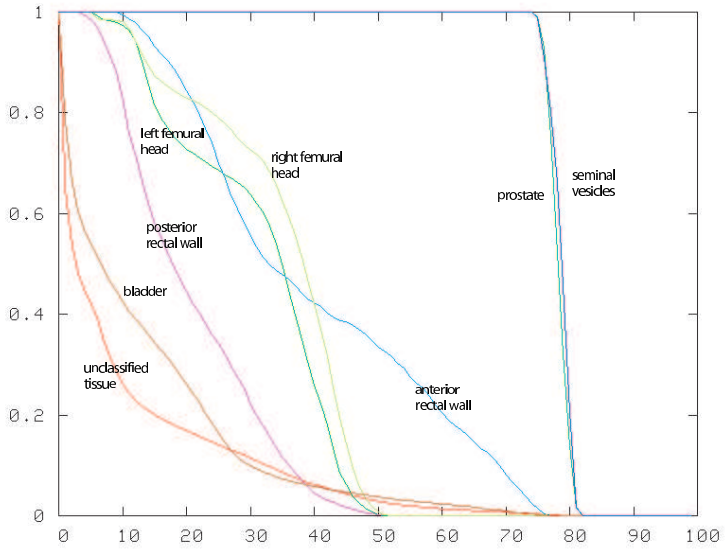

Figure 10: The DVH of the last refinement.

to the femoral heads and the anterior rectal wall. It is evident that the solution using the refinement strategy spared large parts of the anterior rectal wall at the cost of increasing the dose in the femoral heads. As the reference dose for these two organs is rather high compared to the realized dose, this has no effect on the objective function value. To compare, figure 11 displays the normalized EUD values for both, the original solution and the solution obtained from the last refinement.

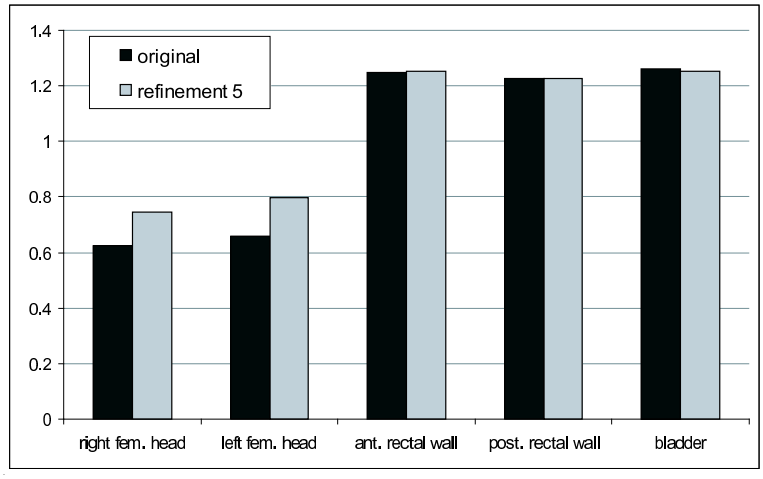

Figure 11: The objective function values (EUDs normalized by their reference doses) for the optimal solution found by the original problem formulation and by the last refinement. The maximum of the values for the optimal solution is obtained by the bladder, and the maximum of the objective function values for the last refinement is given by the value of the anterior rectal wall.

The objective function value for refinement 5 is even slightly better than the solution to the original formulation. This is because the solver stops if no significant improvement can be made for a long time. In the original formulation, the solver may have stopped too early. This shows that the clustering approach may also improve the convergence to the optimal solution.

As may be expected from the quality of the objective function values after the first clustered solution, the normalized EUD values did not change much over the solution process. However, the graphs in figure 12 shows that especially in the first two refinements the biggest improvement of the objective function values was attained by the organ which was refined in that step.

While the original solution took (25+20+20+22+22=) 109 apertures to be delivered, the solution to the last refinement problem took only (25+15+19+19+17=) 95. The number of monitor units, however, was the same at 216.

5 Discussion

In this work we introduced a variable aggregation technique for the treatment planning problem. The aggregation was motivated by a faster dose calculation that would speed up the solver iterations. A disaggregation method motivated by clinically meaningful indicators (i.e. the maximum EUD normalized by the reference dose) was developed to pose adaptively refined versions of the treatment planning

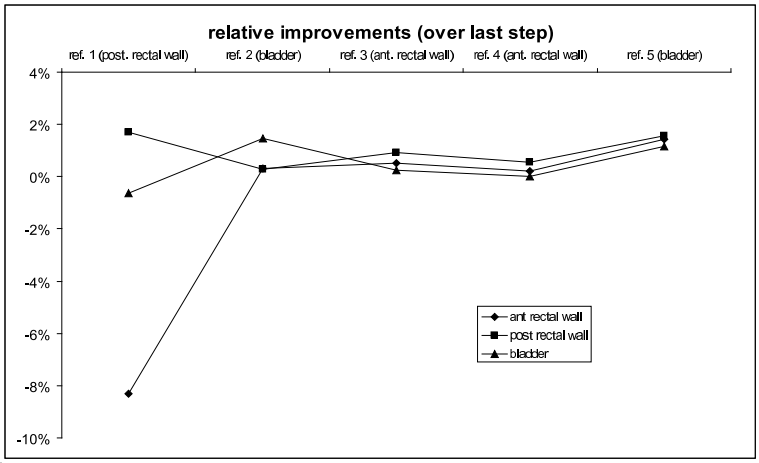

Figure 12: The improvements in the objective functions remained small over the solution process. However, larger improvements were realized for those organs which were chosen for the refinement.

problem. An example calculation on a clinical prostate case demonstrated the potentials of this method. The method introduced found a superior solution in less time. Due to the fact that some beamlets were still in clusters, the solution attained after clustering and refindement also needed significantly fewer shapes after sequencing. The success of this method supports the hypothesis that not all degrees of freedom have to be used to produced treatment plans of high quality.

References

[1] M Alber and F Nüsslin. IMRT optimisation under constraints for static and dynamic MLC delivery. *Physic and Medicine in Biology*, 46(12):3229–3239, 2001.

[2] D Craft, P Süss, and T Bortfeld. The tradeoff between treatment plan quality and intensity field complexity in IMRT. *Submitted to Physics in Medicine and Biology*, 2006.

[3] E Hall. Intensity-modulated radiation therapy, protons, and the risk of second cancers. *Int J Radiation Oncology Biol Phys*, 65(1):1–7, 2006.

[4] J Hartigan. *Clustering Algorithms*. John Wiley & Sons, Inc., 1975.

[5] MA Keller-Reichenbecher, T Bortfeld, S Levegrün, J Stein, K Preiser, and W Schlegel. Intensity modulation with the "step and shoot" technique using a commercial MLC: a planning study. *Int J Radiation Oncology Biol Phys*, 45(5):1315–1324, 1999.

[6] KH Küfer, M Monz, A Scherrer, P Süss, F Alonso, A Azizi Sultan, T Bortfeld, and C Thieke. Multicriteria optimization in intensity modulated radiotherapy planning. In PM Pardalos and HE Romeijn, editors, *Handbook of Optimization in Medicine*, to appear in 2006.

[7] A Niemierko. A generalized concept of equivalent uniform dose (EUD). *Medical Physics*, 26(1):1100, 1999.

[8] A Scherrer, KH Küfer, TR Bortfeld, M Monz, and FV Alonso. IMRT planning on adaptive volume structures - a decisive reduction in computational complexity. *Phys Med Biol*, 50:2033–53, 2005.

[9] W Schlegel and A Mahr. 3D Conformal Radiation Therapy - Multimedia Introduction to Methods and Techniques. Multimedia CD-ROM, Springer, 2001.

[10] C Thieke, T Bortfeld, and KH Küfer. Characterization of dose distributions through the max and mean dose concept. *Acta Oncologica*, 41(2):158–161, 2002.

[11] D Wackerly, W Mendenhall, and R Scheaffer. *Mathematical Statistics with Applications, Sixth Edition*. Duxbury, 2002.

[12] S Webb. *The physics of three-dimensional radiation therapy*. IOP Publishing Ltd, 1993.

[13] S Webb. *The physics of conformal radiotherapy*. IOP Publishing Ltd, 1997.

[14] P Xia and L Verhey. Multileaf collimator leaf-sequencing algorithm for intensity modulated beams with multiple static segments. *Medical Physics*, 25:1424–1434, 1998.

[15] Y Yu. Multiobjective decision theory for computational optimization in radiation therapy. *Medical Physics*, 24:1445–1454, 1997.

Published reports of the Fraunhofer ITWM

The PDF-files of the following reports are available under:
www.itwm.fraunhofer.de/de/zentral__berichte/berichte

1. D. Hietel, K. Steiner, J. Struckmeier
A Finite - Volume Particle Method for Compressible Flows
(19 pages, 1998)

2. M. Feldmann, S. Seibold
Damage Diagnosis of Rotors: Application of Hilbert Transform and Multi-Hypothesis Testing
Keywords: Hilbert transform, damage diagnosis, Kalman filtering, non-linear dynamics
(23 pages, 1998)

3. Y. Ben-Haim, S. Seibold
Robust Reliability of Diagnostic Multi-Hypothesis Algorithms: Application to Rotating Machinery
Keywords: Robust reliability, convex models, Kalman filtering, multi-hypothesis diagnosis, rotating machinery, crack diagnosis
(24 pages, 1998)

4. F.-Th. Lentes, N. Siedow
Three-dimensional Radiative Heat Transfer in Glass Cooling Processes
(23 pages, 1998)

5. A. Klar, R. Wegener
A hierarchy of models for multilane vehicular traffic
Part I: Modeling
(23 pages, 1998)

Part II: Numerical and stochastic investigations
(17 pages, 1998)

6. A. Klar, N. Siedow
Boundary Layers and Domain Decomposition for Radiative Heat Transfer and Diffusion Equations: Applications to Glass Manufacturing Processes
(24 pages, 1998)

7. I. Choquet
Heterogeneous catalysis modelling and numerical simulation in rarified gas flows Part I: Coverage locally at equilibrium
(24 pages, 1998)

8. J. Ohser, B. Steinbach, C. Lang
Efficient Texture Analysis of Binary Images
(17 pages, 1998)

9. J. Orlik
Homogenization for viscoelasticity of the integral type with aging and shrinkage
(20 pages, 1998)

10. J. Mohring
Helmholtz Resonators with Large Aperture
(21 pages, 1998)

11. H. W. Hamacher, A. Schöbel
On Center Cycles in Grid Graphs
(15 pages, 1998)

12. H. W. Hamacher, K.-H. Küfer
Inverse radiation therapy planning - a multiple objective optimisation approach
(14 pages, 1999)

13. C. Lang, J. Ohser, R. Hilfer
On the Analysis of Spatial Binary Images
(20 pages, 1999)

14. M. Junk
On the Construction of Discrete Equilibrium Distributions for Kinetic Schemes
(24 pages, 1999)

15. M. Junk, S. V. Raghurame Rao
A new discrete velocity method for Navier-Stokes equations
(20 pages, 1999)

16. H. Neunzert
Mathematics as a Key to Key Technologies
(39 pages (4 PDF-Files), 1999)

17. J. Ohser, K. Sandau
Considerations about the Estimation of the Size Distribution in Wicksell's Corpuscle Problem
(18 pages, 1999)

18. E. Carrizosa, H. W. Hamacher, R. Klein, S. Nickel
Solving nonconvex planar location problems by finite dominating sets
Keywords: Continuous Location, Polyhedral Gauges, Finite Dominating Sets, Approximation, Sandwich Algorithm, Greedy Algorithm
(19 pages, 2000)

19. A. Becker
A Review on Image Distortion Measures
Keywords: Distortion measure, human visual system
(26 pages, 2000)

20. H. W. Hamacher, M. Labbé, S. Nickel, T. Sonneborn
Polyhedral Properties of the Uncapacitated Multiple Allocation Hub Location Problem
Keywords: integer programming, hub location, facility location, valid inequalities, facets, branch and cut
(21 pages, 2000)

21. H. W. Hamacher, A. Schöbel
Design of Zone Tariff Systems in Public Transportation
(30 pages, 2001)

22. D. Hietel, M. Junk, R. Keck, D. Teleaga
The Finite-Volume-Particle Method for Conservation Laws
(16 pages, 2001)

23. T. Bender, H. Hennes, J. Kalcsics, M. T. Melo, S. Nickel
Location Software and Interface with GIS and Supply Chain Management
Keywords: facility location, software development, geographical information systems, supply chain management
(48 pages, 2001)

24. H. W. Hamacher, S. A. Tjandra
Mathematical Modelling of Evacuation Problems: A State of Art
(44 pages, 2001)

25. J. Kuhnert, S. Tiwari
Grid free method for solving the Poisson equation
Keywords: Poisson equation, Least squares method, Grid free method
(19 pages, 2001)

26. T. Götz, H. Rave, D. Reinel-Bitzer, K. Steiner, H. Tiemeier
Simulation of the fiber spinning process
Keywords: Melt spinning, fiber model, Lattice Boltzmann, CFD
(19 pages, 2001)

27. A. Zemitis
On interaction of a liquid film with an obstacle
Keywords: impinging jets, liquid film, models, numerical solution, shape
(22 pages, 2001)

28. I. Ginzburg, K. Steiner
Free surface lattice-Boltzmann method to model the filling of expanding cavities by Bingham Fluids
Keywords: Generalized LBE, free-surface phenomena, interface boundary conditions, filling processes, Bingham viscoplastic model, regularized models
(22 pages, 2001)

29. H. Neunzert
»Denn nichts ist für den Menschen als Menschen etwas wert, was er nicht mit Leidenschaft tun kann«
Vortrag anlässlich der Verleihung des Akademiepreises des Landes Rheinland-Pfalz am 21.11.2001
Keywords: Lehre, Forschung, angewandte Mathematik, Mehrskalenanalyse, Strömungsmechanik
(18 pages, 2001)

30. J. Kuhnert, S. Tiwari
Finite pointset method based on the projection method for simulations of the incompressible Navier-Stokes equations
Keywords: Incompressible Navier-Stokes equations, Meshfree method, Projection method, Particle scheme, Least squares approximation
AMS subject classification: 76D05, 76M28
(25 pages, 2001)

31. R. Korn, M. Krekel
Optimal Portfolios with Fixed Consumption or Income Streams
Keywords: Portfolio optimisation, stochastic control, HJB equation, discretisation of control problems.
(23 pages, 2002)

32. M. Krekel
Optimal portfolios with a loan dependent credit spread
Keywords: Portfolio optimisation, stochastic control, HJB equation, credit spread, log utility, power utility, non-linear wealth dynamics
(25 pages, 2002)

33. J. Ohser, W. Nagel, K. Schladitz
The Euler number of discretized sets – on the choice of adjacency in homogeneous lattices
Keywords: image analysis, Euler number, neighborhod relationships, cuboidal lattice
(32 pages, 2002)

34. I. Ginzburg, K. Steiner

Lattice Boltzmann Model for Free-Surface flow and Its Application to Filling Process in Casting

Keywords: Lattice Boltzmann models; free-surface phenomena; interface boundary conditions; filling processes; injection molding; volume of fluid method; interface boundary conditions; advection-schemes; upwind-schemes
(54 pages, 2002)

35. M. Günther, A. Klar, T. Materne, R. Wegener

Multivalued fundamental diagrams and stop and go waves for continuum traffic equations

Keywords: traffic flow, macroscopic equations, kinetic derivation, multivalued fundamental diagram, stop and go waves, phase transitions
(25 pages, 2002)

36. S. Feldmann, P. Lang, D. Prätzel-Wolters

Parameter influence on the zeros of network determinants

Keywords: Networks, Equicofactor matrix polynomials, Realization theory, Matrix perturbation theory
(30 pages, 2002)

37. K. Koch, J. Ohser, K. Schladitz

Spectral theory for random closed sets and estimating the covariance via frequency space

Keywords: Random set, Bartlett spectrum, fast Fourier transform, power spectrum
(28 pages, 2002)

38. D. d'Humières, I. Ginzburg

Multi-reflection boundary conditions for lattice Boltzmann models

Keywords: lattice Boltzmann equation, boudary condistions, bounce-back rule, Navier-Stokes equation
(72 pages, 2002)

39. R. Korn

Elementare Finanzmathematik

Keywords: Finanzmathematik, Aktien, Optionen, Portfolio-Optimierung, Börse, Lehrerweiterbildung, Mathematikunterricht
(98 pages, 2002)

40. J. Kallrath, M. C. Müller, S. Nickel

Batch Presorting Problems: Models and Complexity Results

Keywords: Complexity theory, Integer programming, Assigment, Logistics
(19 pages, 2002)

41. J. Linn

On the frame-invariant description of the phase space of the Folgar-Tucker equation

Key words: fiber orientation, Folgar-Tucker equation, injection molding
(5 pages, 2003)

42. T. Hanne, S. Nickel

A Multi-Objective Evolutionary Algorithm for Scheduling and Inspection Planning in Software Development Projects

Key words: multiple objective programming, project management and scheduling, software development, evolutionary algorithms, efficient set
(29 pages, 2003)

43. T. Bortfeld , K.-H. Küfer, M. Monz, A. Scherrer, C. Thieke, H. Trinkaus

Intensity-Modulated Radiotherapy - A Large Scale Multi-Criteria Programming Problem

Keywords: multiple criteria optimization, representative systems of Pareto solutions, adaptive triangulation, clustering and disaggregation techniques, visualization of Pareto solutions, medical physics, external beam radiotherapy planning, intensity modulated radiotherapy
(31 pages, 2003)

44. T. Halfmann, T. Wichmann

Overview of Symbolic Methods in Industrial Analog Circuit Design

Keywords: CAD, automated analog circuit design, symbolic analysis, computer algebra, behavioral modeling, system simulation, circuit sizing, macro modeling, differential-algebraic equations, index
(17 pages, 2003)

45. S. E. Mikhailov, J. Orlik

Asymptotic Homogenisation in Strength and Fatigue Durability Analysis of Composites

Keywords: multiscale structures, asymptotic homogenization, strength, fatigue, singularity, non-local conditions
(14 pages, 2003)

46. P. Domínguez-Marín, P. Hansen, N. Mladenovi´c , S. Nickel

Heuristic Procedures for Solving the Discrete Ordered Median Problem

Keywords: genetic algorithms, variable neighborhood search, discrete facility location
(31 pages, 2003)

47. N. Boland, P. Domínguez-Marín, S. Nickel, J. Puerto

Exact Procedures for Solving the Discrete Ordered Median Problem

Keywords: discrete location, Integer programming
(41 pages, 2003)

48. S. Feldmann, P. Lang

Padé-like reduction of stable discrete linear systems preserving their stability

Keywords: Discrete linear systems, model reduction, stability, Hankel matrix, Stein equation
(16 pages, 2003)

49. J. Kallrath, S. Nickel

A Polynomial Case of the Batch Presorting Problem

Keywords: batch presorting problem, online optimization, competetive analysis, polynomial algorithms, logistics
(17 pages, 2003)

50. T. Hanne, H. L. Trinkaus

knowCube for MCDM – Visual and Interactive Support for Multicriteria Decision Making

Key words: Multicriteria decision making, knowledge management, decision support systems, visual interfaces, interactive navigation, real-life applications.
(26 pages, 2003)

51. O. Iliev, V. Laptev

On Numerical Simulation of Flow Through Oil Filters

Keywords: oil filters, coupled flow in plain and porous media, Navier-Stokes, Brinkman, numerical simulation
(8 pages, 2003)

52. W. Dörfler, O. Iliev, D. Stoyanov, D. Vassileva

On a Multigrid Adaptive Refinement Solver for Saturated Non-Newtonian Flow in Porous Media

Keywords: Nonlinear multigrid, adaptive refinement, non-Newtonian flow in porous media
(17 pages, 2003)

53. S. Kruse

On the Pricing of Forward Starting Options under Stochastic Volatility

Keywords: Option pricing, forward starting options, Heston model, stochastic volatility, cliquet options
(11 pages, 2003)

54. O. Iliev, D. Stoyanov

Multigrid – adaptive local refinement solver for incompressible flows

Keywords: Navier-Stokes equations, incompressible flow, projection-type splitting, SIMPLE, multigrid methods, adaptive local refinement, lid-driven flow in a cavity
(37 pages, 2003)

55. V. Starikovicius

The multiphase flow and heat transfer in porous media

Keywords: Two-phase flow in porous media, various formulations, global pressure, multiphase mixture model, numerical simulation
(30 pages, 2003)

56. P. Lang, A. Sarishvili, A. Wirsen

Blocked neural networks for knowledge extraction in the software development process

Keywords: Blocked Neural Networks, Nonlinear Regression, Knowledge Extraction, Code Inspection
(21 pages, 2003)

57. H. Knaf, P. Lang, S. Zeiser

Diagnosis aiding in Regulation Thermography using Fuzzy Logic

Keywords: fuzzy logic,knowledge representation, expert system
(22 pages, 2003)

58. M. T. Melo, S. Nickel, F. Saldanha da Gama

Largescale models for dynamic multicommodity capacitated facility location

Keywords: supply chain management, strategic planning, dynamic location, modeling
(40 pages, 2003)

59. J. Orlik

Homogenization for contact problems with periodically rough surfaces

Keywords: asymptotic homogenization, contact problems
(28 pages, 2004)

60. A. Scherrer, K.-H. Küfer, M. Monz, F. Alonso, T. Bortfeld

IMRT planning on adaptive volume structures – a significant advance of computational complexity

Keywords: Intensity-modulated radiation therapy (IMRT), inverse treatment planning, adaptive volume structures, hierarchical clustering, local refinement, adaptive clustering, convex programming, mesh generation, multi-grid methods
(24 pages, 2004)

61. D. Kehrwald

Parallel lattice Boltzmann simulation of complex flows

Keywords: Lattice Boltzmann methods, parallel computing, microstructure simulation, virtual material design, pseudo-plastic fluids, liquid composite moulding
(12 pages, 2004)

62. O. Iliev, J. Linn, M. Moog, D. Niedziela, V. Starikovicius

On the Performance of Certain Iterative Solvers for Coupled Systems Arising in Discretization of Non-Newtonian Flow Equations

Keywords: Performance of iterative solvers, Preconditioners, Non-Newtonian flow
(17 pages, 2004)

63. R. Ciegis, O. Iliev, S. Rief, K. Steiner

On Modelling and Simulation of Different Regimes for Liquid Polymer Moulding

Keywords: Liquid Polymer Moulding, Modelling, Simulation, Infiltration, Front Propagation, non-Newtonian flow in porous media
(43 pages, 2004)

64. T. Hanne, H. Neu

Simulating Human Resources in Software Development Processes

Keywords: Human resource modeling, software process, productivity, human factors, learning curve
(14 pages, 2004)

65. O. Iliev, A. Mikelic, P. Popov

Fluid structure interaction problems in deformable porous media: Toward permeability of deformable porous media

Keywords: fluid-structure interaction, deformable porous media, upscaling, linear elasticity, stokes, finite elements
(28 pages, 2004)

66. F. Gaspar, O. Iliev, F. Lisbona, A. Naumovich, P. Vabishchevich

On numerical solution of 1-D poroelasticity equations in a multilayered domain

Keywords: poroelasticity, multilayered material, finite volume discretization, MAC type grid
(41 pages, 2004)

67. J. Ohser, K. Schladitz, K. Koch, M. Nöthe

Diffraction by image processing and its application in materials science

Keywords: porous microstructure, image analysis, random set, fast Fourier transform, power spectrum, Bartlett spectrum
(13 pages, 2004)

68. H. Neunzert

Mathematics as a Technology: Challenges for the next 10 Years

Keywords: applied mathematics, technology, modelling, simulation, visualization, optimization, glass processing, spinning processes, fiber-fluid interaction, trubulence effects, topological optimization, multicriteria optimization, Uncertainty and Risk, financial mathematics, Malliavin calculus, Monte-Carlo methods, virtual material design, filtration, bio-informatics, system biology
(29 pages, 2004)

69. R. Ewing, O. Iliev, R. Lazarov, A. Naumovich

On convergence of certain finite difference discretizations for 1D poroelasticity interface problems

Keywords: poroelasticity, multilayered material, finite volume discretizations, MAC type grid, error estimates
(26 pages,2004)

70. W. Dörfler, O. Iliev, D. Stoyanov, D. Vassileva

On Efficient Simulation of Non-Newtonian Flow in Saturated Porous Media with a Multigrid Adaptive Refinement Solver

Keywords: Nonlinear multigrid, adaptive renement, non-Newtonian in porous media
(25 pages, 2004)

71. J. Kalcsics, S. Nickel, M. Schröder

Towards a Unified Territory Design Approach – Applications, Algorithms and GIS Integration

Keywords: territory desgin, political districting, sales territory alignment, optimization algorithms, Geographical Information Systems
(40 pages, 2005)

72. K. Schladitz, S. Peters, D. Reinel-Bitzer, A. Wiegmann, J. Ohser

Design of acoustic trim based on geometric modeling and flow simulation for non-woven

Keywords: random system of fibers, Poisson line process, flow resistivity, acoustic absorption, Lattice-Boltzmann method, non-woven
(21 pages, 2005)

73. V. Rutka, A. Wiegmann

Explicit Jump Immersed Interface Method for virtual material design of the effective elastic moduli of composite materials

Keywords: virtual material design, explicit jump immersed interface method, effective elastic moduli, composite materials
(22 pages, 2005)

74. T. Hanne

Eine Übersicht zum Scheduling von Baustellen

Keywords: Projektplanung, Scheduling, Bauplanung, Bauindustrie
(32 pages, 2005)

75. J. Linn

The Folgar-Tucker Model as a Differetial Algebraic System for Fiber Orientation Calculation

Keywords: fiber orientation, Folgar–Tucker model, invariants, algebraic constraints, phase space, trace stability
(15 pages, 2005)

76. M. Speckert, K. Dreßler, H. Mauch, A. Lion, G. J. Wierda

Simulation eines neuartigen Prüfsystems für Achserprobungen durch MKS-Modellierung einschließlich Regelung

Keywords: virtual test rig, suspension testing, multibody simulation, modeling hexapod test rig, optimization of test rig configuration
(20 pages, 2005)

77. K.-H. Küfer, M. Monz, A. Scherrer, P. Süss, F. Alonso, A. S. A. Sultan, Th. Bortfeld, D. Craft, Chr. Thieke

Multicriteria optimization in intensity modulated radiotherapy planning

Keywords: multicriteria optimization, extreme solutions, real-time decision making, adaptive approximation schemes, clustering methods, IMRT planning, reverse engineering
(51 pages, 2005)

78. S. Amstutz, H. Andrä

A new algorithm for topology optimization using a level-set method

Keywords: shape optimization, topology optimization, topological sensitivity, level-set
(22 pages, 2005)

79. N. Ettrich

Generation of surface elevation models for urban drainage simulation

Keywords: Flooding, simulation, urban elevation models, laser scanning
(22 pages, 2005)

80. H. Andrä, J. Linn, I. Matei, I. Shklyar, K. Steiner, E. Teichmann

OPTCAST – Entwicklung adäquater Strukturoptimierungsverfahren für Gießereien Technischer Bericht (KURZFASSUNG)

Keywords: Topologieoptimierung, Level-Set-Methode, Gießprozesssimulation, Gießtechnische Restriktionen, CAE-Kette zur Strukturoptimierung
(77 pages, 2005)

81. N. Marheineke, R. Wegener

Fiber Dynamics in Turbulent Flows Part I: General Modeling Framework

Keywords: fiber-fluid interaction; Cosserat rod; turbulence modeling; Kolmogorov's energy spectrum; double-velocity correlations; differentiable Gaussian fields

Part II: Specific Taylor Drag

Keywords: flexible fibers; k-ε turbulence model; fiber-turbulence interaction scales; air drag; random Gaussian aerodynamic force; white noise; stochastic differential equations; ARMA process
(38 pages, 2005)

82. C. H. Lampert, O. Wirjadi

An Optimal Non-Orthogonal Separation of the Anisotropic Gaussian Convolution Filter

Keywords: Anisotropic Gaussian filter, linear filtering, orientation space, nD image processing, separable filters
(25 pages, 2005)

83. H. Andrä, D. Stoyanov

Error indicators in the parallel finite element solver for linear elasticity DDFEM

Keywords: linear elasticity, finite element method, hierarchical shape functions, domain decom-position, parallel implementation, a posteriori error estimates
(21 pages, 2006)

84. M. Schröder, I. Solchenbach

Optimization of Transfer Quality in Regional Public Transit

Keywords: public transit, transfer quality, quadratic assignment problem
(16 pages, 2006)

85. A. Naumovich, F. J. Gaspar

On a multigrid solver for the three-dimensional Biot poroelasticity system in multilayered domains

Keywords: poroelasticity, interface problem, multigrid, operator-dependent prolongation
(11 pages, 2006)

86. S. Panda, R. Wegener, N. Marheineke

Slender Body Theory for the Dynamics of Curved Viscous Fibers

Keywords: curved viscous fibers; fluid dynamics; Navier-Stokes equations; free boundary value problem; asymptotic expansions; slender body theory
(14 pages, 2006)

87. E. Ivanov, H. Andrä, A. Kudryavtsev

Domain Decomposition Approach for Automatic Parallel Generation of Tetrahedral Grids

Key words: Grid Generation, Unstructured Grid, Delaunay Triangulation, Parallel Programming, Domain Decomposition, Load Balancing
(18 pages, 2006)

88. S. Tiwari, S. Antonov, D. Hietel, J. Kuhnert, R. Wegener

A Meshfree Method for Simulations of Interactions between Fluids and Flexible Structures

Key words: Meshfree Method, FPM, Fluid Structure Interaction, Sheet of Paper, Dynamical Coupling
(16 pages, 2006)

89. R. Ciegis , O. Iliev, V. Starikovicius, K. Steiner

Numerical Algorithms for Solving Problems of Multiphase Flows in Porous Media

Keywords: nonlinear algorithms, finite-volume method, software tools, porous media, flows
(16 pages, 2006)

90. D. Niedziela, O. Iliev, A. Latz

On 3D Numerical Simulations of Viscoelastic Fluids

Keywords: non-Newtonian fluids, anisotropic viscosity, integral constitutive equation
(18 pages, 2006)

91. A. Winterfeld

Application of general semi-infinite Programming to Lapidary Cutting Problems

Keywords: large scale optimization, nonlinear programming, general semi-infinite optimization, design centering, clustering
(26 pages, 2006)

92. J. Orlik, A. Ostrovska

Space-Time Finite Element Approximation and Numerical Solution of Hereditary Linear Viscoelasticity Problems

Keywords: hereditary viscoelasticity; kern approximation by interpolation; space-time finite element approximation, stability and a priori estimate
(24 pages, 2006)

93. V. Rutka, A. Wiegmann, H. Andrä

EJIIM for Calculation of effective Elastic Moduli in 3D Linear Elasticity

Keywords: Elliptic PDE, linear elasticity, irregular domain, finite differences, fast solvers, effective elastic moduli
(24 pages, 2006)

94. A. Wiegmann, A. Zemitis

EJ-HEAT: A Fast Explicit Jump Harmonic Averaging Solver for the Effective Heat Conductivity of Composite Materials

Keywords: Stationary heat equation, effective thermal conductivity, explicit jump, discontinuous coefficients, virtual material design, microstructure simulation, EJ-HEAT
(21 pages, 2006)

95. A. Naumovich

On a finite volume discretization of the three-dimensional Biot poroelasticity system in multilayered domains

Keywords: Biot poroelasticity system, interface problems, finite volume discretization, finite difference method.
(21 pages, 2006)

96. M. Krekel, J. Wenzel

A unified approach to Credit Default Swaption and Constant Maturity Credit Default Swap valuation

Keywords: LIBOR market model, credit risk, Credit Default Swaption, Constant Maturity Credit Default Swap-method.
(43 pages, 2006)

97. A. Dreyer

Interval Methods for Analog Circiuts

Keywords: interval arithmetic, analog circuits, tolerance analysis, parametric linear systems, frequency response, symbolic analysis, CAD, computer algebra
(36 pages, 2006)

98. N. Weigel, S. Weihe, G. Bitsch, K. Dreßler

Usage of Simulation for Design and Optimization of Testing

Keywords: Vehicle test rigs, MBS, control, hydraulics, testing philosophy
(14 pages, 2006)

99. H. Lang, G. Bitsch, K. Dreßler, M. Speckert

Comparison of the solutions of the elastic and elastoplastic boundary value problems

Keywords: Elastic BVP, elastoplastic BVP, variational inequalities, rate-independency, hysteresis, linear kinematic hardening, stop- and play-operator
(21 pages, 2006)

100. M. Speckert, K. Dreßler, H. Mauch

MBS Simulation of a hexapod based suspension test rig

Keywords: Test rig, MBS simulation, suspension, hydraulics, controlling, design optimization
(12 pages, 2006)

101. S. Azizi Sultan, K.-H. Küfer

A dynamic algorithm for beam orientations in multicriteria IMRT planning

Keywords: radiotherapy planning, beam orientation optimization, dynamic approach, evolutionary algorithm, global optimization
(14 pages, 2006)

102. T. Götz, A. Klar, N. Marheineke, R. Wegener

A Stochastic Model for the Fiber Lay-down Process in the Nonwoven Production

Keywords: fiber dynamics, stochastic Hamiltonian system, stochastic averaging
(17 pages, 2006)

103. Ph. Süss, K.-H. Küfer

Balancing control and simplicity: a variable aggregation method in intensity modulated radiation therapy planning

Keywords: IMRT planning, variable aggregation, clustering methods
(22 pages, 2006)

Status quo: November 2006